Analysis of a Power Conditioning System for Superconducting Magnetic Energy Storage (SMES)

D. Casadei, G. Grandi, U. Reggiani, G. Serra

Department of Electrical Engineering
University of Bologna
Viale Risorgimento 2, Bologna 40136
Italy
elettrot5@dns.ing.unibo.it

Abstract - A Power Conditioning System (PCS) which can be utilized for the compensation of non-linear and pulsating loads is analyzed in this paper. The PCS consists of a voltage source inverter and a dc current chopper, and uses a SMES as energy storage device. The whole system is controlled by three regulators acting on the superconducting coil stored energy, the dc-link voltage, and the inverter ac currents. Numerical simulations have been carried out by PSpice to verify the performance of the PCS in different operating conditions.

I. INTRODUCTION

In recent years many papers which analyze the potential applications of SMES systems to utilities have been presented, and different converter topologies have been proposed [1]-[9]. A typical configuration of a SMES power conditioning system consists of a superconducting magnet and a set of power converters. The SMES connected to a power system network is capable of controlling the active and reactive power simultaneously. This control capability can be utilized to meet a variety of applications, including power system stabilization, diurnal load-leveling, static VAR compensation, current harmonic compensation, and Uninterruptable Power Supply (UPS) applications.

The energy storage system based on Superconducting Coils (SCs) offers several advantages with respect to traditional chemical storage devices (batteries). In particular, the SMES can be charged and discharged very fast allowing high power demands to be satisfied with comparably low stored energy. In addition, very high energy densities [J/m^3] can be achieved and several charging and discharging cycles are possible without known limits.

In [8] and [9] current source and voltage source converter topologies have been compared and current converters have been considered as the best solution in order to get a fast transfer of active and reactive power into the network. The power converter based on SCR line-commutated bridge rectifier has limitations such as lagging power factor and significant low-order current harmonics. The Total Harmonic Distortion (THD) even using the twelve-pulse topology is too high to comply with harmonic standards.

To overcome these limits, it is possible to use converters based on self-commutating devices such as GTO or IGBT. Using these devices, a PWM control strategy can be carried out improving the low-order harmonic content and reducing the requirement for ac-line filters. This solution can be employed for power factor correction, fluctuating load compensation and UPS. It should be noted that these features can be met also using Voltage Source Inverters (VSIs). In addition, this converter topology has the inherent capability to operate as a shunt active filter.

It is known that non-linear loads, such as static power converters, cause undesirable phenomena in the operation of power systems. Among these, one of the most important is the harmonic pollution. Various active power filter configurations and control strategies have been proposed [10]-[13], but shunt active filters have been recognized as the viable solution to current harmonic compensation. In order to provide this last feature, the PCS considered in this paper has a topology including a voltage source inverter and a two-quadrant current chopper, as represented in Fig. 1. The two converters are decoupled by a dc-link. The SC is characterized by a relatively large inductance and behaves as a constant dc current source.

The chopper operates in order to control the capacitor voltage of the dc-link. The inverter acts as interface between the dc-link and the ac power supply, controlling the compensating currents flowing through the series ac-link inductors.

It should be noted that, in order to meet the above mentioned features, a pulsed operation of the SC is required,

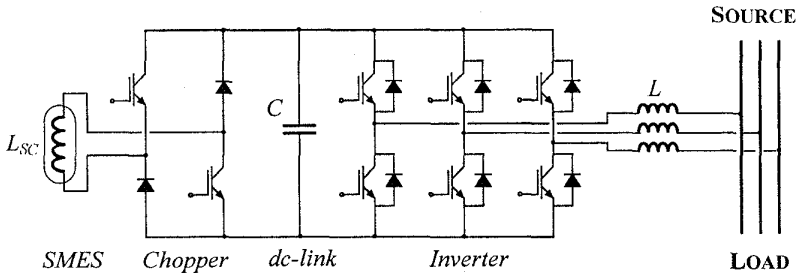

Fig. 1. Schematic drawing of the PCS structure

0-7803-4756-0/98/$10.00 1998 IEEE

causing ac current losses. These losses must be taken into account when designing the SMES refrigeration system.

This paper presents a complete control system which is able to satisfy, at the same time, the requirements of shunt active filters and power conditioners. The control system is composed of three independent regulators which are designed in order to keep under control the SC energy, the dc-link voltage, and the VSI ac currents. A detailed analysis is carried out for each regulator, determining the transfer function and showing the influence of the regulator parameters. Numerical simulations have been performed considering non-linear and pulsating loads. In particular, a three-phase full bridge rectifier supplying a resistive-inductive load has been considered as non-linear load. The results obtained show that the proposed control system is able to satisfy the requirements of power conditioners and active filters.

II. PRINCIPLE OF OPERATION

For the analytical developments, the three-phase quantities are represented with space vectors according to a stationary *d-q* transformation defined as

$$\bar{x} = x_d + j x_q = \sqrt{\frac{2}{3}}\left(x_a + x_b e^{j\frac{2}{3}\pi} + x_c e^{j\frac{4}{3}\pi}\right) \qquad (1)$$

The behavior of the PCS is determined by three closed-loop regulators, as represented in the block diagram of Fig. 2. The first regulator controls the SC energy, the second one the dc-link voltage and the third one the VSI ac currents.

The basic principle of the control system is to impose sinusoidal source currents in phase with the corresponding line-to-neutral source voltages. Then, the reference value of the source current is represented by the current space vector $\bar{i}_S^*$ in phase with the source voltage space vector $\bar{v}_S$. The source current magnitude I_s^* is obtained by the regulator R_1, acting on the instantaneous error between the reference value of the SC energy E_{SC}^* and its actual value E_{SC}, being $E_{SC} = \frac{1}{2} L_{SC} I_{SC}^2$. The regulator R_1 operates in order to keep the SC energy close to its reference value.

The two-quadrant chopper performs a PWM current control by the regulator R_2. In this way the dc-link voltage V_C is kept close to its reference value V_C^* and the energy stored in the capacitor is nearly constant. Thus, the active power is flowing directly from the supply to the SMES (with exception of the switch and inductor losses).

The control system requires the measurement of the load current $\bar{i}_L$, which is used to calculate the reference value of the filter current $\bar{i}_F^*$ as follows

$$\bar{i}_F^* = \bar{i}_S^* - \bar{i}_L . \qquad (2)$$

The value of $\bar{i}_F^*$ is the input command for the inverter and can be utilized to implement both hysteresis or PWM current regulators. If the filter current $\bar{i}_F$ is measured, a hysteresis current regulator acting on the instantaneous current error $\Delta\bar{i}_F = \bar{i}_F^* - \bar{i}_F$ can be employed to determine the inverter switch states S_A, S_B, S_C. Alternatively, a PWM current regulator can be used avoiding the drawbacks of hysteresis current controllers. In this case, the reference voltage for the inverter can be calculated by the voltage equation written across the link inductance L. Neglecting the resistive effects, this equation yields

$$\bar{v}_S = \bar{v}_F + L\frac{d\bar{i}_F}{dt} . \qquad (3)$$

Using a variational model, the reference inverter voltage $\bar{v}_F^*$ can be expressed as a function of the instantaneous filter current error by

$$\bar{v}_F^* = \bar{v}_S - \frac{L}{\Delta t}\Delta\bar{i}_F . \qquad (4)$$

It can be noticed that, usually, the ac inverter current $\bar{i}_F$ is also measured for diagnostic and protection purposes. Then, hysteresis and the PWM current regulators based on the measurement of the load and filter currents are widely used. However, the control system could be implemented with the load current measurement only. In fact, a different procedure can be adopted to calculate the inverter reference voltage $\bar{v}_F^*$, as described in [14].

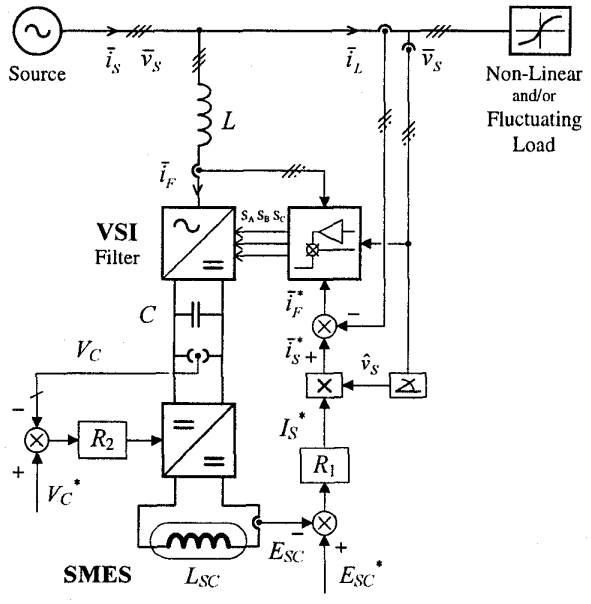

Fig. 2. Block diagram of the PCS control scheme

III. ANALYSIS OF THE CONTROL LOOPS

The power conditioning system analyzed in this paper should be designed in order to satisfy the requirements related to various tasks, in different frequency ranges,

- reduction of flicker («50 Hz)
- current harmonic compensation (»50 Hz)
- reactive power compensation (50-60 Hz)
- uninterruptable power supply (50-60 Hz).

The flicker phenomena are generated by the presence of pulsating loads which cause distortions and fluctuations of the line currents. This, owing to the line impedance, pro-

duces changes in the supply voltages. The reduction of flicker can be achieved using the PCS to deliver the alternating component of the load power. The performance of the compensator is determined by the rating of the converter and the SMES, and by the characteristics of the regulator which performs the SC energy storage control. In general, the time response of this control loop is several cycle periods (i.e., hundreds of ms).

With reference to the dc-link voltage, we can observe that the control loop should keep the voltage level close to its reference value. In this way, the VSI operates correctly regardless of the stored energy in the SC.

Transient changes in the instantaneous power absorbed by the load generates voltage fluctuations across the dc capacitor. These voltage fluctuations depend on the dc-link capacitor and the regulator parameters, and should be smoothed within few cycle periods (i.e., tens of ms).

In order to compensate reactive power and current harmonics of non-linear loads, the PCS must operate as an active filter. According to their principle of operation, the parallel active filters behave as harmonic current sources. Then, the implementation of suitable current regulators is required. The dynamic behavior of the active filter, for a prefixed dc-voltage, is mainly affected by the time response of the ac current control loop, which must be fast enough to track the reference current waveforms closely (i.e., fractions of ms).

Then, the three regulators have different features, requiring quite different time responses. Thus, they can be designed as three independent control loops.

A. SC Energy Control Loop

The dynamic behavior of the SC energy control loop is investigated with reference to the block diagram of Fig. 3.

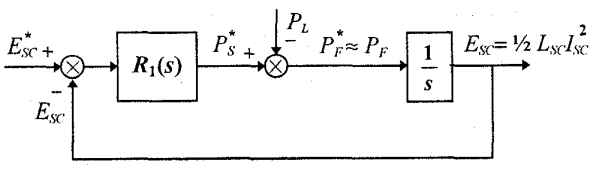

Fig. 3. Block diagram of the SC energy control loop

The input of the regulator R_1 is the error of the SC stored energy, the output is the reference value of the source power P_S^* defined as $P_S^* = V_s I_s^*$. The reference value of the power absorbed by the filter P_F^* is calculated by subtracting the load power P_L to P_S^*. Assuming that the PWM inverter is able to generate the reference power at each cycle period, yields $P_F = P_F^*$. This instantaneous power represents the total power flowing from the supply to the PCS. Neglecting the rate of change of the magnetic energy in the link inductors, P_F represents the input power to the VSI. Furthermore, the dc-link voltage can be considered constant, being the dc-link control loop faster than the SC energy control loop. As a consequence, neglecting the losses of the two converters, the energy stored in the SC (E_{sc}) is given by the time integral of P_F.

Under these assumptions, the following expression can be derived from the block diagram represented in Fig. 3

$$E_{SC} = \frac{R_1(s)}{s + R_1(s)} E^*_{SC} - \frac{1}{s + R_1(s)} P_L \qquad (5)$$

As (5) shows, the load power P_L represents a perturbation in the SC energy control loop. The effect of this perturbation is determined by the type of regulator, i.e., by the expression $R_1(s)$.

The aim of this control loop is to smooth the load power fluctuation which determine the flicker phenomena. The relationship between the load power and the source power is expressed by

$$P_S = \frac{R_1(s)}{s + R_1(s)} P_L \qquad (6)$$

It can be noticed that the dynamic relationship between P_L and P_S is the same as between E^*_{SC} and E_{SC}.

The choice of the regulator R_1 must be made taking the PCS features into account. In particular, depending on weather the PCS is used as UPS or not, a different behavior is required. When the PCS is used only for the compensation of current harmonics and pulsating loads, the regulator can be implemented by a simple proportional gain, i.e., $R_1(s)=K_p$. In this case, (5) becomes

$$E_{SC} = \frac{1}{1+\tau s} E^*_{SC} - \frac{\tau}{1+\tau s} P_L \qquad (7)$$

The first term in (7) represents the low-pass filtering action applied to E^*_{SC} with the time constant $\tau=1/K_p$. The second term shows the influence of the load power, introducing a steady-state error in the stored energy. With the proportional regulator the PCS operates correctly, delivering or absorbing energy in response to load changes, and the value of the stored energy never exceeds the reference value. The value of K_p represents the cut-off angular frequency ($1/\tau$) and defines the bandwidth of the low-pass filtering action that the PCS introduces between P_L and P_S. By selecting a cut-off frequency of few Hertz it is possible to compensate the power fluctuation and the corresponding voltage flicker. The minimum flicker frequency which has to be compensated, together with the maximum power of the load, can be utilized to determine the rated storage energy in the SC.

An alternative solution is to consider as regulator a low-pass filter, i.e., $R_1(s)=K_p/(1+\tau s)$. In this case, second order transfer functions are obtained, leading to

$$E_{SC} = \frac{\omega_n^2}{s^2 + 2\delta\omega_n s + \omega_n^2} E^*_{SC} - \frac{\frac{1}{K_p}\omega_n^2(1+\tau s)}{s^2 + 2\delta\omega_n s + \omega_n^2} P_L \qquad (8)$$

where $\omega_n = \sqrt{\frac{K_p}{\tau}}$ and $\delta = \frac{1}{2}\frac{1}{\sqrt{K_p \tau}}$.

A smoothed response can be achieved by choosing $\delta > 1$. Also in this case, the load power introduces a steady-state error in the stored energy.

The behavior obtained by these two regulators is not satisfactory if the PCS is employed as UPS. In fact, the requirement for UPS operation is to keep the stored energy always close to its reference value, so that the PCS is able

to satisfy the load power demand in all the time periods in which the network is down. In order to satisfy this feature, the regulator must introduce an integral action. Then, assuming for $R_1(s)$ a PI regulator, expressed as

$$R_1(s) = K_p\left(1+\frac{1}{T_i s}\right) = K_p\frac{1+T_i s}{T_i s} \tag{9}$$

leads to

$$E_{SC} = \frac{\omega_n^2(1+T_i s)}{s^2+2\delta\omega_n s+\omega_n^2}E_{SC}^* - \frac{\frac{T_i}{K_p}\omega_n^2 s}{s^2+2\delta\omega_n s+\omega_n^2}P_L \text{ , } \tag{10}$$

where $\omega_n = \sqrt{\frac{K_p}{T_i}}$ and $\delta = \frac{1}{2}\sqrt{K_p T_i}$.

By (10) it is possible to verify that the load power does not introduce steady-state errors in the SC stored energy. Therefore, in response to load changes, the regulator acts in order to recover the reference value of the SC energy.

B. DC-Link Voltage Control Loop

The analysis of the dc-link voltage regulator is carried out with reference to the control scheme represented in Fig. 4.

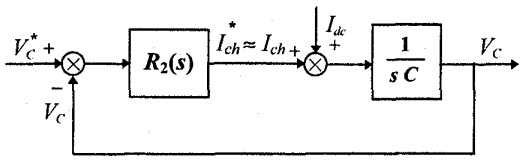

Fig. 4. Block diagram of the dc-link voltage control loop

The input of the regulator R_2 is the dc-link voltage error, the output is the reference value of the chopper current I_{ch}^*. In this case, the perturbation is represented by the dc-side current of the VSI, I_{dc}. From the block diagram of Fig. 4, the following transfer function can be obtained

$$V_C = \frac{R_2(s)}{sC+R_2(s)}V_C^* + \frac{1}{sC+R_2(s)}I_{dc} \text{ .} \tag{11}$$

In this case, the dc-link voltage must be regulated to its reference value to ensure a correct operation of the inverter. Then, a PI regulator is chosen for $R_2(s)$ to accomplish the system requirements yielding

$$R_2(s) = K_p\left(1+\frac{1}{T_i s}\right) = K_p\frac{1+T_i s}{T_i s} \text{ .} \tag{12}$$

Introducing (12) in (11) leads to

$$V_C = \frac{\omega_n^2(1+T_i s)}{s^2+2\delta\omega_n s+\omega_n^2}V_C^* + \frac{\frac{T_i}{K_p}\omega_n^2 s}{s^2+2\delta\omega_n s+\omega_n^2}I_{dc} \tag{13}$$

where $\omega_n = \sqrt{\frac{K_p}{T_i C}}$ and $\delta = \frac{1}{2}\sqrt{\frac{T_i K_p}{C}}$.

Eq. 13 shows that the dc inverter current does not introduce steady-state errors in the dc voltage. With the same assumptions made in the previous section, the dc-side inverter current can be expressed as

$$I_{dc} \approx \frac{P_F}{V_C} \text{ .} \tag{14}$$

Then, the relationship between the dc link voltage and the filter power is

$$V_C^2 = \frac{\frac{T_i}{K_p}\omega_n^2 s}{s^2+2\delta\omega_n s+\omega_n^2}P_F \text{ .} \tag{15}$$

C. AC Currents Control Loop

The ac-side inverter currents are controlled according to the block diagram shown in Fig. 5. The inverter reference voltage is determined on the basis of (4) leading to

$$\bar{v}_F^* = \bar{v}_S - K_p\Delta\bar{i}_F \text{ .} \tag{16}$$

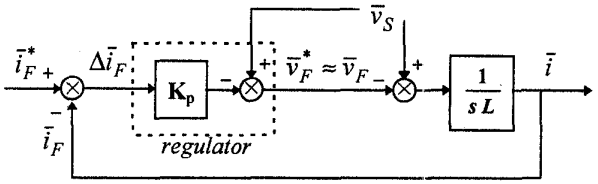

Fig. 5. Block diagram of the filter ac current control loop

In this case, the control is performed by a feed-forward compensation of the source voltage and by a simple proportional gain. With reference to Fig. 5, it is possible to determine the transfer function of the closed loop system. If we assume that the PWM inverter is able to generate the reference voltage at each cycle period, the following equation is obtained

$$\bar{i}_F = \frac{1}{1+\tau s}\bar{i}_F^* \text{ , where } \tau = \frac{L}{K_p} \text{.} \tag{17}$$

Eq. 17 shows that the response of the ac current loop is represented by a simple first order low-pass filter. As it could be expected, the time constant τ is proportional to the ac-link inductance L, but the effect of this inductance can be compensated by selecting a suitable value for K_p. However, the dynamic performance of the control loop cannot be improved indefinitely, being the inverter output voltage limited by the dc-link voltage.

III. SIMULATION RESULTS

In order to verify the dynamic performance of the PCS, two different models have been implemented using PSpice. The former considers both the inverter and the chopper as ideal converters, i.e. neglecting the switching effects. Under this assumption the electrical quantities are represented by their averaged values. This simplified model requires very low computational times (few tens of seconds) and can be employed to adjust the parameters of the system regulators. The latter is implemented considering the power IGBT as ideal switches, i.e., with instantaneous lossless commutations. In this case the electrical quantities obtained by the numerical simulations are expected to be very close to the corresponding real quantities containing the switching harmonics.

The numerical simulations have been carried out with reference to a three-phase, 380 V, 50 Hz, supply system.
The utility interface characteristics depend on the leakage reactance of the transformer connected in the point of common coupling, which is assumed 0.04 p.u.. In these conditions the total source inductance is L_S =100μH. The parameters of the power conditioning system are given in Tab. I. The gains of the regulators have been chosen in order to obtain the required values for the time constants, damping factor and bandwidth, as shown in Tab. II.

TAB. I - MAIN PARAMETERS OF THE PCS

ac-link inductance, L	0.5 mH
dc-link capacitor, C	10 mF
dc-link rated voltage, V_C^*	800 V
SC rated energy, E_{SC}^*	50 kJ
SC rated current, I_{SC}^*	500 A
SC inductance, L_{SC}	0.4 H

TAB. II - REGULATOR GAINS

SC ENERGY REGULATOR	
τ= 100 ms	K_p=10 s^{-1}

DC-LINK VOLTAGE REGULATOR	
T_i=16 ms , δ=2	K_p=10 Ω^{-1}

AC CURRENT REGULATOR	
Bandwidth=20 kHz	K_p=63 Ω

The first simulation has been carried out in order to test the SC energy control loop during the switch-on and the switch-off of a 200 kW linear load. For this analysis it is not necessary to consider the switching effects, so that the simplified model can be utilized.
Fig. 6 illustrates the results obtained for load current, source current, load and source power, and SC current. As fig. 6 shows, the step changes of the load power are smoothed by the PCS. During the switch-on the PCS delivers the difference between P_L and P_S , and the SC current decreases. The reference value of I_{SC} is recovered as the load is switched-off. According to the analysis developed in Section III.*A*, a simple proportional regulator has been utilized for this application and the results obtained are in agreement with (6) and (7). The PCS capability of compensating flicker phenomena has been verified considering the linear load pulsating with a frequency of 5 Hz. The same regulator as in the previous simulation has been utilized. The results obtained are illustrated in Fig. 7. Analyzing the smoothed variations of the source power, and the behavior of the SC current, it is evident that the PCS operates in order to deliver the difference between the load power and its average value.
A further simulation has been carried out using the model which takes the switching effects into account. This simulation aims to verify the PCS performance when the current harmonics of a non-linear load must be compensated. To this end, a three-phase, 380 V, 50 Hz, full bridge rectifier supplying a 200 kW resistive-inductive load has been considered. The results obtained are illustrated in Fig. 8. This figure clearly shows that the PCS is able to compensate the low frequency current harmonics. It can be noted that the higher frequency harmonics generated by the current commutations in the bridge diodes cannot be completely compensated.

IV. CONCLUSIONS

A new control scheme for power conditioning systems, in which a SMES is employed to obtain high energy storage capability, has been analyzed in this paper. The use of a two-quadrant dc chopper, connecting the SMES to the dc-side of the voltage source inverter, allows frequent charging and discharging cycles of the superconducting coil. The control scheme has been tested in different operating conditions by numerical simulations. For this purpose, both simplified and detailed models have been implemented by PSpice. In this way, the dynamic behavior of the whole system can be verified with good accuracy and reasonable computational times. The proposed control scheme is very simple to be implemented and the results obtained have demonstrated its capability to compensate non-linear and pulsating loads.

V. REFERENCES

[1] H.J. Boeing, J.F. Hauer, "Commissioning Test of the Bonneville Power Administration 30 MJ Superconducting Magnetic Energy Storage Unit," IEEE Trans. on PAS, Vol. 104, pp. 302-312, February 1985.

[2] R.L. Kustom, J.J. Skiles, J. Wang, "Power Conversion System for Diurnal Load Levelling with Superconducting Magnetic Energy Storage," IEEE trans. on Magnetics, Vol. 23, September 1987.

[3] R.L. Lasseter, S.G. Jalai, "Dynamic Response of Power Conditioning Systems for Superconductive Magnetic Energy Storage," IEEE Trans. Energy Conversion, Vol. 6, pp. 388-393, September 1991.

[4] R.L. Kustom, J.J. Skiles, J. Wang, K. Klontz, T. Ise, K. Ko, F. Vong, "Research on Power Conditioning Systems for Superconductive Magnetic Energy Storage (SMES)," IEEE Trans. on Magnetics, Vol. 27, pp. 2320-2323, March 1991.

[5] I. D. Hassan, R.M. Bucci, K.T. Swe, "400MW SMES Power Conditioning System Development and Simulation," IEEE Trans. Power Electronics, Vol. 8, pp. 237-249, July 1993.

[6] M. Tada, Y. Mitani, K. Tsuji, " Power Control by Superconducting Magnetic Energy Storage for Load Change Compensation and Power System Stabilization in Interconnected Power System," IEEE Trans. on Applied Superconductivity, Vol. 5, pp. 250-253, June 1995.

[7] J.J. Skiles, R.L. Kustom, K. Ko, "Performance of a Power Conversion System for Superconducting Magnetic Energy Storage (SMES)," IEEE Trans. on Power Systems, Vol. 11, pp. 1718-1723, November 1996.

[8] I.J. Iglesias, J. Acero, A. Bautista, "Comparative Study and Simulation of Optimal Converter Topologies for SMES Systems," IEEE Trans. on Applied Superconductivity, Vol. 5, pp. 254-257, June 1995.

[9] I. J. Iglesias, A. Bautista, M. Visiers, "Experimental and Simulated Results of a SMES Fed by a Current Source Inverter," IEEE Trans. on Applied Superconductivity, Vol. 7, pp.861-864, June 1997.

[10] L.Gyugyi, E.C.Strycula, "Active AC Power Filter," Proc. IEEE-IAS Annual Meeting, pp. 529, 1976.

[11] H.Akagi, Y.Kanazawa, A.Nabae, "Instantaneous Reactive Power Compensators Comprising Switching Devices without Energy Storage Components," IEEE Trans. on IA, Vol. 20, pp. 625, 1984.

[12] L.Malesani, L.Rossetto, P.Tenti, "Active Filters for Reactive Power and Harmonic Compensation," Proc. IEEE-PESC, pp. 321-330, June 1986.

[13] O. Simon, H. Spaeth, K.P. Juengst, P. Komarek, "Experimental Setup of a Shunt Active Filter Using a Superconducting Magnetic Energy Storage Device," Proc. EPE'97, Vol.1, pp. 447-452, September 1997.

[14] U. Reggiani, D. Casadei, G. Grandi, "Active Power Filters Based on a Single Current Measurement System," SPEEDAM'98 Conference, Sorrento (IT), June 3-5, 1998.

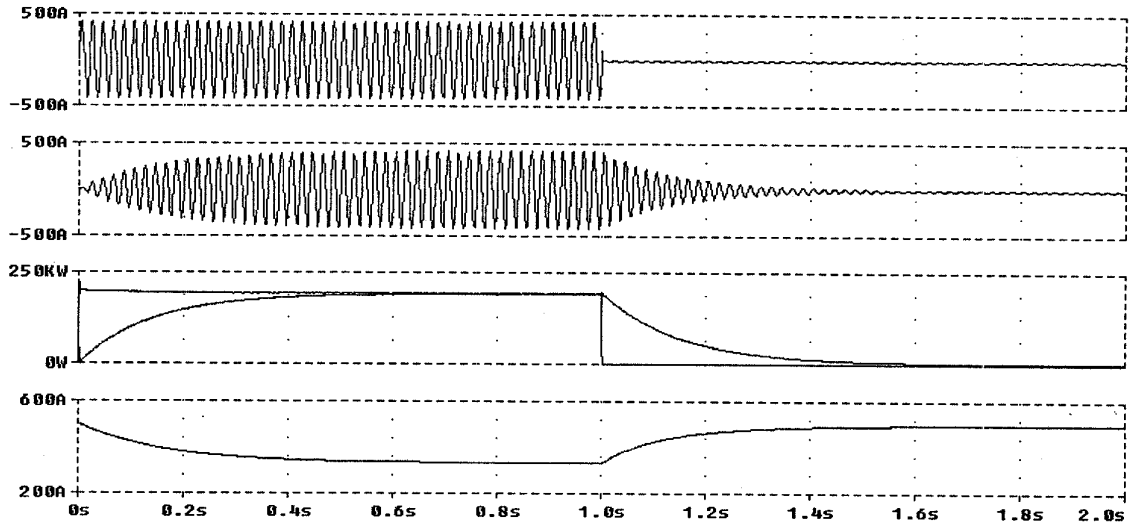

Fig. 6. Switch-on and switch-off of a 200 kW linear load. From top to bottom: load current, source current, load and source power, SC current.

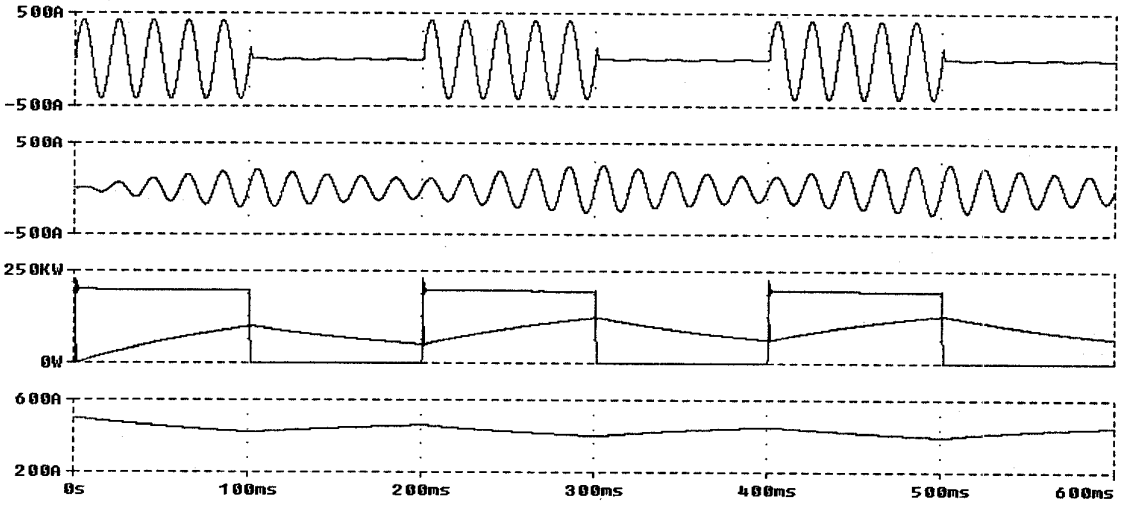

Fig. 7. Linear load pulsating with a frequency of 5 Hz. From top to bottom: load current, source current, load and source power, SC current.

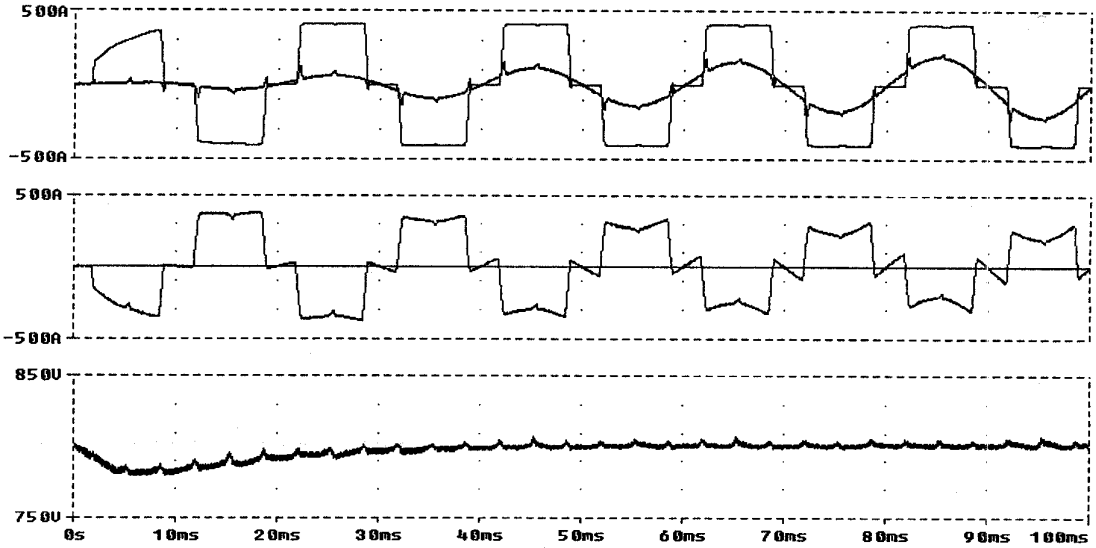

Fig. 8. Full bridge rectifier supplying a 200 kW R-L load. From top to bottom: load and source currents, filter current, dc-link voltage.